AD-A091 980 SRI INTERNATIONAL MENLO PARK CA F/G 4/1
BACKSCATTER MEASUREMENTS OF 11-CM EQUATORIAL SPREAD-F IRREGULAR--ETC(U)
JUN 80 R T TSUNODA DNA001-79-C-0153
UNCLASSIFIED DNA-5324T NL

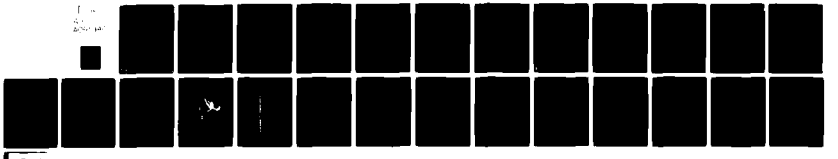

END
DATE FILMED
8 81
DTIC

DNA 5324T

BACKSCATTER MEASUREMENTS OF 11-cm EQUATORIAL SPREAD-F IRREGULARITIES

Roland T. Tsunoda
SRI International
333 Ravenswood Avenue
Menlo Park, California 94025

1 June 1980

Topical Report 5 for Period 1 October 1979—1 November 1979

CONTRACT No. DNA 001-79-C-0153

THIS WORK SPONSORED BY THE DEFENSE NUCLEAR AGENCY
UNDER RDT&E RMSS CODE B322079462 I25AAXHX64009 H2590D.

Prepared for
Director
DEFENSE NUCLEAR AGENCY
Washington, D. C. 20305

Destroy this report when it is no longer needed. Do not return to sender.

PLEASE NOTIFY THE DEFENSE NUCLEAR AGENCY, ATTN: STTI, WASHINGTON, D.C. 20305, IF YOUR ADDRESS IS INCORRECT, IF YOU WISH TO BE DELETED FROM THE DISTRIBUTION LIST, OR IF THE ADDRESSEE IS NO LONGER EMPLOYED BY YOUR ORGANIZATION.

UNCLASSIFIED

SECURITY CLASSIFICATION OF THIS PAGE (When Data Entered)

REPORT DOCUMENTATION PAGE

READ INSTRUCTIONS BEFORE COMPLETING FORM

1. REPORT NUMBER: DNA 5324T	2. GOVT ACCESSION NO.: AD-A091 980
3. RECIPIENT'S CATALOG NUMBER: no.	
4. TITLE (and Subtitle): BACKSCATTER MEASUREMENTS OF 11-cm EQUATORIAL SPREAD-F IRREGULARITIES	5. TYPE OF REPORT & PERIOD COVERED: Topical Report 5, for Period 1 Oct [illegible] -1 Nov 79
	6. PERFORMING ORG. REPORT NUMBER: SRI Project 8164
7. AUTHOR(s): Roland T. Tsunoda	8. CONTRACT OR GRANT NUMBER(s): Contract DNA001-79-C-0153
9. PERFORMING ORGANIZATION NAME AND ADDRESS: SRI International, 333 Ravenswood Avenue, Menlo Park, California 94025	10. PROGRAM ELEMENT, PROJECT, TASK AREA & WORK UNIT NUMBERS: Subtask I25AAXHX640-09
11. CONTROLLING OFFICE NAME AND ADDRESS: Director, Defense Nuclear Agency, Washington, D.C. 20305	12. REPORT DATE: 1 June 1980 / 13. NUMBER OF PAGES: 26
14. MONITORING AGENCY NAME & ADDRESS (if different from Controlling Office)	15. SECURITY CLASS (of this report): UNCLASSIFIED
	15a. DECLASSIFICATION/DOWNGRADING SCHEDULE

16. DISTRIBUTION STATEMENT (of this Report)

Approved for public release; distribution unlimited.

17. DISTRIBUTION STATEMENT (of the abstract entered in Block 20, if different from Report)

18. SUPPLEMENTARY NOTES

This work sponsored by the Defense Nuclear Agency under RDT&E RMSS Code B322079462 I25AAXHX64009 H2590D.

19. KEY WORDS (Continue on reverse side if necessary and identify by block number)

Equatorial spread F
Plasma bubbles
Ionospheric irregularities

20. ABSTRACT (Continue on reverse side if necessary and identify by block number)

An important objective of the Defense Nuclear Agency is to understand the physical processes that control the dissipation of turbulent structure in plasmas. Such turbulent structures occur as a consequence of high-altitude nuclear events as well as in the natural, disturbed equatorial ionosphere. Analysis and understanding of those processes in the nighttime equatorial F-region ionosphere that are analogous to those found in the nuclear environment can lead to an intelligent extrapolation of equatorial findings to the → next page

DD FORM 1 JAN 73 1473 EDITION OF 1 NOV 68 IS OBSOLETE

UNCLASSIFIED

SECURITY CLASSIFICATION OF THIS PAGE (When Data Entered)

40281 Job

20. ABSTRACT (Continued)

nuclear case. In the equatorial F-region ionosphere, the turbulent cascade process had been found previously to extend from irregularity spatial wavelengths longer than tens of kilometers down to wavelengths as short as 36 cm. To investigate the small-scale regime of wavelengths less than 36 cm, a radar backscatter experiment was conducted in the Kwajalein Atoll, Marshall Islands using a frequency that corresponds to an irregularity wavelength of 11 cm.

The first observations of radar backscatter from 11-cm equatorial field-aligned irregularities (FAI) are described. These measurements extend the spatial wavelength regime of F-region FAI to lengths that approach both the electron gyroradius and the Debye length. Agreement of these results with the theory of high-frequency drift waves suggests that these observations may be unique to the equatorial ionosphere. That is, the requirement for low electron densities that the theory calls for may preclude the existence of 11-cm FAI elsewhere in the F-region ionosphere, except in equatorial plasma bubbles.

PREFACE

The author would like to thank the TRADEX and ALTAIR staffs for their support during this experiment. The author also thanks Dr. G. Ahlgren (MIT/Lincoln Laboratory) for providing in-the-field data analysis support including the TRADEX results presented in this report.

CONTENTS

ILLUSTRATIONS

TABLE

I INTRODUCTION

During July 1979, a coordinated field program was sponsored by the Defense Nuclear Agency to investigate the phenomena of equatorial spread F. The experiment included the use of two high-power backscatter radars, ALTAIR and TRADEX, located in the Kwajalein Atoll, Marshall Islands. ALTAIR operates at 155.5 MHz and 415 MHz, and has been used previously to characterize the 1-m and 36-cm field-aligned irregularities (FAI) that produce the backscatter at those frequencies [e.g., Tsunoda et al., 1979; Towle, 1980; Tsunoda, 1980c]. TRADEX was employed for the first time in this kind of experiment to extend radar observations of equatorial FAI to 1320 MHz, the highest frequency ever used. Backscatter at this frequency corresponds to an FAI wavelength of 11 cm.

A primary objective of extending radar observations to higher frequencies is to seek the "inner scale" of equatorial plasma turbulence. That is, TRADEX measurements were directed toward answering the question, "what is the smallest wavelength at which equatorial FAI can exist?"

The background of radar backscatter observations of equatorial FAI and the rationale for interest in characterizing the small-scale end of the FAI power spectrum is given in Section II. The experiment utilizing both ALTAIR and TRADEX radars is described in Section III, and the preliminary results are presented in Section IV. In Section V, the results are discussed in relation to an existing plasma instability model that has been proposed as the source mechanism for these small-scale FAI that exist, with spatial wavelengths, below the ion gyroradius [Huba et al., 1978].

II BACKGROUND

Radar backscatter has been used to study equatorial spread-F irregularities for more than four decades, first in the form of vertical-incidence ionosondes [Booker and Wells, 1938] and high-frequency (HF) backscatter radars [Clemesha, 1964; Kelleher and Skinner, 1971], and most recently in the form of high-power backscatter radars that operate in the very-high-frequency (VHF) and ultra-high-frequency (UHF) bands [Farley et al., 1970; Woodman and La Hoz, 1976; Tsunoda et al., 1979; Towle, 1980]. A characteristic trend apparent in these measurements is the use of increasingly higher transmitter power at higher radar frequencies. The need for increased radar sensitivity underscores the waning strength of these FAI as their spatial wavelength decreases.

The implied decrease in FAI strength with decreasing spatial wavelengths is not surprising. Measurements of the power spectral density associated with larger-scale ($\gtrsim$ 1 km) equatorial irregularities have already indicated a power-law dependence on spatial wavelength [e.g., Basu et al., 1976]. It is by no means apparent, however, that the rate of decrease (characterized by a power-law spectral index) in FAI strength should be constant over the entire range of spatial wavelengths. In fact, it is perhaps natural to expect significant decreases in FAI strength when the FAI spatial wavelength becomes comparable to or less than the characteristic plasma scale lengths. Drastic decreases (or "cutoffs") in FAI strength might be envisioned whether we think in terms of an "inner scale" to a spectrum of turbulence, or whether we consider source mechanisms for FAI generation and growth.

For example, intuitively, it is apparent that gradients in plasma density do not produce rapid growth of irregularities when the wavelength is much smaller than the gradient scale length. It is also apparent that gradients or irregularities in plasma density are

difficult to maintain if their scale sizes are comparable to (or less than) the ion or electron gyroradius. This happens because we can no longer treat particle motion by its "guiding center." And finally, any organized motion involving electrons and ions is not possible at spatial distances less than the Debye length. From these heuristic arguments, we might expect possible cutoffs in FAI strength at spatial wavelengths comparable to (1) the ion gyroradius, (2) the electron gyroradius, or (3) the Debye length.

The largest of the three characteristic lengths in ionospheric plasma is the ion gyroradius. The nighttime equatorial F-layer ionosphere typically consists of O^+ ions at a temperature of 1000K. For this case, the ion gyroradius is 5.6 m. Irregularities with this spatial wavelength produce radar backscatter at a frequency of 26.8 MHz. On this basis, radar backscatter at frequencies above 26.8 MHz (which includes all of the VHF and UHF bands) must occur from FAI with spatial wavelengths less than the ion gyroradius.

Woodman and Basu [1978] considered the possible existence of a cutoff in FAI strength near the ion gyroradius. They compared in-situ measurements of large-scale FAI to 50-MHz backscatter strength and found that 3-m FAI was much weaker in strength than expected from extrapolation of the large-scale FAI strength using the observed power-law dependence of the in-situ irregularity spectrum. They suggested that an explanation for this discrepancy might be a cutoff in FAI strength near the ion gyroradius. Since then, however, Tsunoda et al. [1979] and Towle [1980] have pointed out that the Woodman and Basu model, which contains a Gaussian-shaped cutoff near the ion gyroradius precludes the existence of 1-m and 36-cm FAI. Observations of 1-m and 36-cm FAI by Tsunoda et al. [1979] and Towle [1980] refute the accuracy of the Gaussian cutoff model. These observations do not, however, shed further light on the nature of FAI strength dependence on spatial wavelength near to or less than the ion gyroradius.

With the demonstrated existence of radar backscatter from FAI as short as 36 cm, Huba et al. [1978] proposed that high-frequency drift

waves driven by the lower-hybrid-drift instability could account for these small-scale FAI. In their model, Huba et al. [1978] assume that $k^2r_i^2 \gg 1$ and find that maximum linear growth rates occur near $kr_e \sim 1$, where k is the wave number and r_i (r_e) is the ion (electron) gyroradius. For an electron temperature of 1000 K, r_e in the equatorial ionosphere is 3.3 cm. Consequently, their model predicts maximum growth rate for FAI with a spatial wavelength of 20.7 cm, and probably strong backscatter at the corresponding radar frequency of 725 MHz.

The condition $k^2r_i^2 \gg 1$ implies damping of this instability at the longer wavelengths that approach the ion gyroradius. Huba and Ossakow [1979] and Goldman and Sperling [1979] have shown that electron viscosity (from electron-electron collisions) can control the growth of FAI at the short wavelength end of the spectrum. A detailed analysis is required to determine whether the cutoff occurs at wavelengths that approach the electron gyroradius.

Even as we approach the electron gyroradius, we need to consider the effects produced by proximity to the Debye length. This is particularly true in the case of the lower-hybrid-drift instability because electron viscosity is small when the plasma density is low. That is, low plasma densities favor growth of high-frequency drift waves [e.g., Huba and Ossakow, 1979]. Experimentally, Tsunoda [1980a and b] and Szuszczewicz et al. [1980] have shown that small-scale FAI are spatially coincident with large-scale (tens of km) plasma depletions, or "bubbles" [Hanson and Sanatani, 1973; McClure et al., 1977], that exist in the equatorial ionosphere. The plasma density within these bubbles has been found as low as 10^3 el/cm^3. For an electron temperature of 1000 K, the Debye length would be 6.9 cm. Therefore, dissipative effects on FAI growth may be compounded at wavelengths that approach the Debye length.

To the author's knowledge, a source mechanism that produces FAI with spatial wavelengths in the range between the electron gyroradius and the Debye length has never been proposed.

III THE EXPERIMENT

The experiment to detect the existence of 11-cm FAI was conducted on Roi-Namur Island in the Kwajalein Atoll, Marshall Islands. Two high-power radars were used: ALTAIR (ARPA Long-Range Tracking and Instrumentation Radar) and the TRADEX (Target Resolution and Discrimination Experiments) radar. Both are support radars for the Kwajalein Missile Range under the technical supervision of MIT Lincoln Laboratory. ALTAIR is a fully steerable backscatter radar that operates at two frequencies, 155.5 MHz (VHF) and 415 MHz (UHF), simultaneously. ALTAIR has been the source of all observations of equatorial FAI with spatial wavelengths of 1 m and 36 cm. TRADEX is also a fully steerable backscatter radar. It operates at 1320 MHz (L band) and is located within a hundred meters of ALTAIR. The pertinent ALTAIR and TRADEX radar parameters are listed in Table 1.

Table 1

RADAR SYSTEMS CHARACTERISTICS

PARAMETERS	VALUE	
	ALTAIR	TRADEX
Frequency, MHz	415	1320
Peak power, MW	20	4
Pulse width, μs	40	50/1.7 μs (Chirp)
Antenna:		
Diameter, m (ft)	45.7 (150)	25.6 (84)
Beamwidth, deg	1.1	0.65
Gain, dB	42.4	48.5
Effective Aperture, m^2	722	283
Temperature, K	785	622
Polarization	LC/RC	LC/RC

Tsunoda et al. [1979] and Towle [1980] have shown that ALTAIR is sensitive enough to perform incoherent-scatter (IS) measurements at both VHF and UHF. Consequently, ALTAIR is easily capable of detecting backscatter from FAI. On the other hand, TRADEX with its extremely short transmitted waveform is less sensitive than ALTAIR, and is not capable (as configured) of IS measurements. In fact, because of the very short pulse width, the TRADEX sensitivity is considered marginal for detection of 11-cm FAI. For example, if we assume a wavelength dependence of FAI of $\lambda^{2.3}$ (inferred from past ALTAIR data), we expect detectable backscatter with TRADEX only under the most disturbed spread-F conditions.

Because of the marginal TRADEX sensitivity, the experiment was conducted as follows. ALTAIR was operated in a continuous (magnetic) east-west scan, maintaining the radar beam perpendicular to the geomagnetic field lines at F-region altitudes. TRADEX was kept in a standby mode during the ALTAIR scans. TRADEX was turned on and operated only when strong backscatter was observed with ALTAIR at UHF.

The procedure for directing the TRADEX antenna beam to the region of strong UHF backscatter consisted of storing the ALTAIR beam position at which the strong backscatter was observed. That position was selected in real time during an ALTAIR scan by pushing a "zap" button. TRADEX was then immediately directed to the zap coordinates and operated in a limited elevation scan. The elevation scan consisted of seven discrete beam positions with the center position at the zap point. The beam positions were spaced in elevation at intervals of half a beamwidth ($\sim$0.3°). Data were recorded at each beam position for 1 min at a PRF of 125 s^{-1}, thereby completing a scan in 7 min.

TRADEX data were taken at 150-m range intervals to maintain the range resolution (and backscatter detectability) of the 1.7-μs chirp waveform. To reduce the high data rates, 1024 range samples were recorded beginning at a start range that was specified in real time to match the altitude interval of the strong UHF backscatter. In this burst sampling mode, TRADEX data taken over any selected 153-km range interval could be recorded.

This dual-radar experiment was conducted as a part of a larger coordinated rocket program (designed to investigate equatorial spread-F phenomena), sponsored by the Defense Nuclear Agency. Data were collected over a two-week period in mid-July 1979.

IV RESULTS

For this short report, a data set obtained on 17 July 1979 between 1102 UT and 1110 UT (2212 to 2220 local solar time) was selected. During this period, ALTAIR backscatter approached 50 dB above IS levels at VHF and 40 dB above IS levels at UHF. The backscatter strengths are some of the strongest observed with ALTAIR. (In comparison, the Jicamarca 50-MHz radar has observed backscatter strengths up to about 50 dB above IS levels; see Woodman and Basu [1978].)

The backscatter distribution observed with ALTAIR at UHF is shown in Figure 1. The backscatter strength is represented by contours of constant signal strength (after range-squared correction). The contours, shown in decade increments of backscatter strength, are calibrated with reference to IS signal strength. The zero dB contour is equivalent to IS from an electron density of 10^6 el/cm^3. In this map, the altitude-modulated bottomside backscatter is centered around the 350-km altitude and backscatter "plumes" extend upward from the bottomside into the topside of the F layer. (Tsunoda [1980c] presents the basis for these inferences.) The intense, altitude-extended plume just west of ALTAIR contains the region of interest.

The TRADEX line-of-sight (LOS), also shown in Figure 1, passes through the intense backscatter plume mapped by ALTAIR. The white bar located just beyond the arrow head on the LOS vector shows the range extent from which L-band backscatter was observed and coincides with a region of strong UHF backscatter ($\gtrsim$30 dB).

Figure 2 shows the TRADEX measurements made along the LOS in Figure 1. In the upper panel, we have displayed the backscatter strength versus range record obtained by time averaging the TRADEX data for one minute. The range resolution is 150 m with this kind of data processing. The lower panel contains the same backscatter profile after range-averaging to simulate the ALTAIR range resolution of

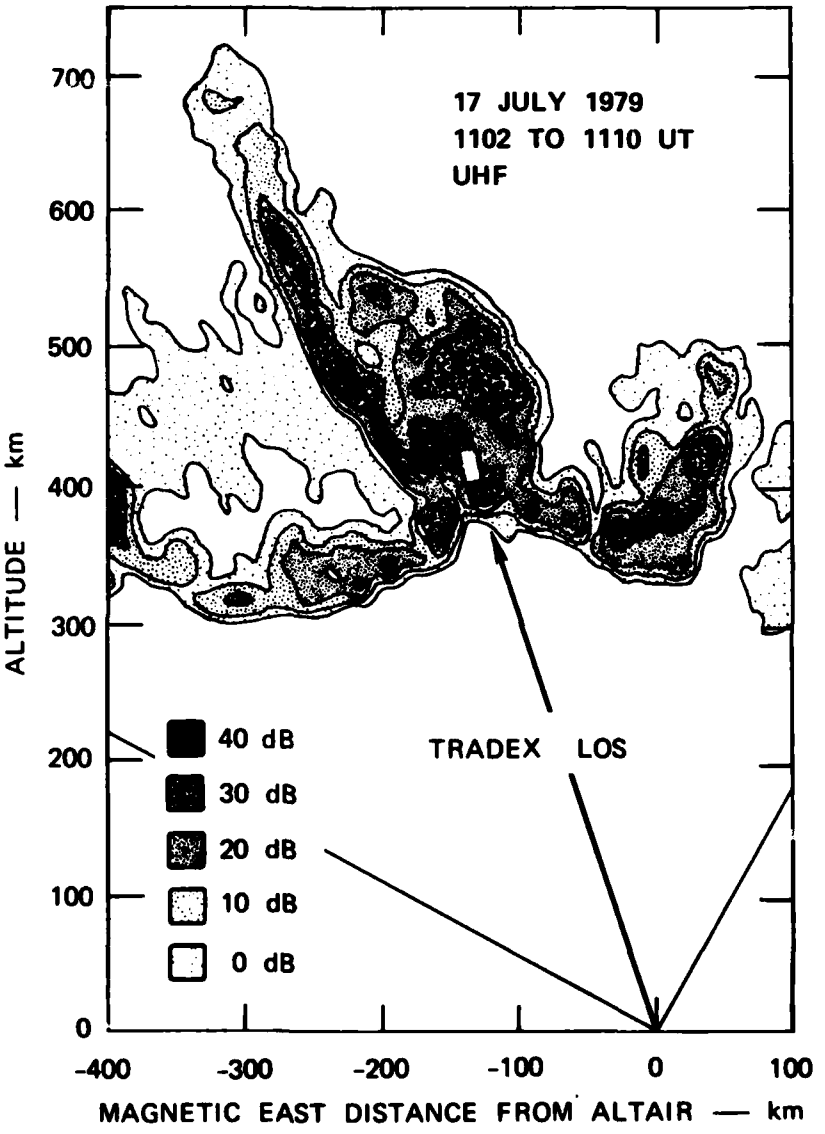

FIGURE 1 SPATIAL DISTRIBUTION OF RADAR BACKSCATTER FROM EQUATORIAL FAI OBTAINED AT 415 MHz WITH ALTAIR. The TRADEX radar line-of-sight (LOS) vector points to region of backscatter at 1320 MHz.

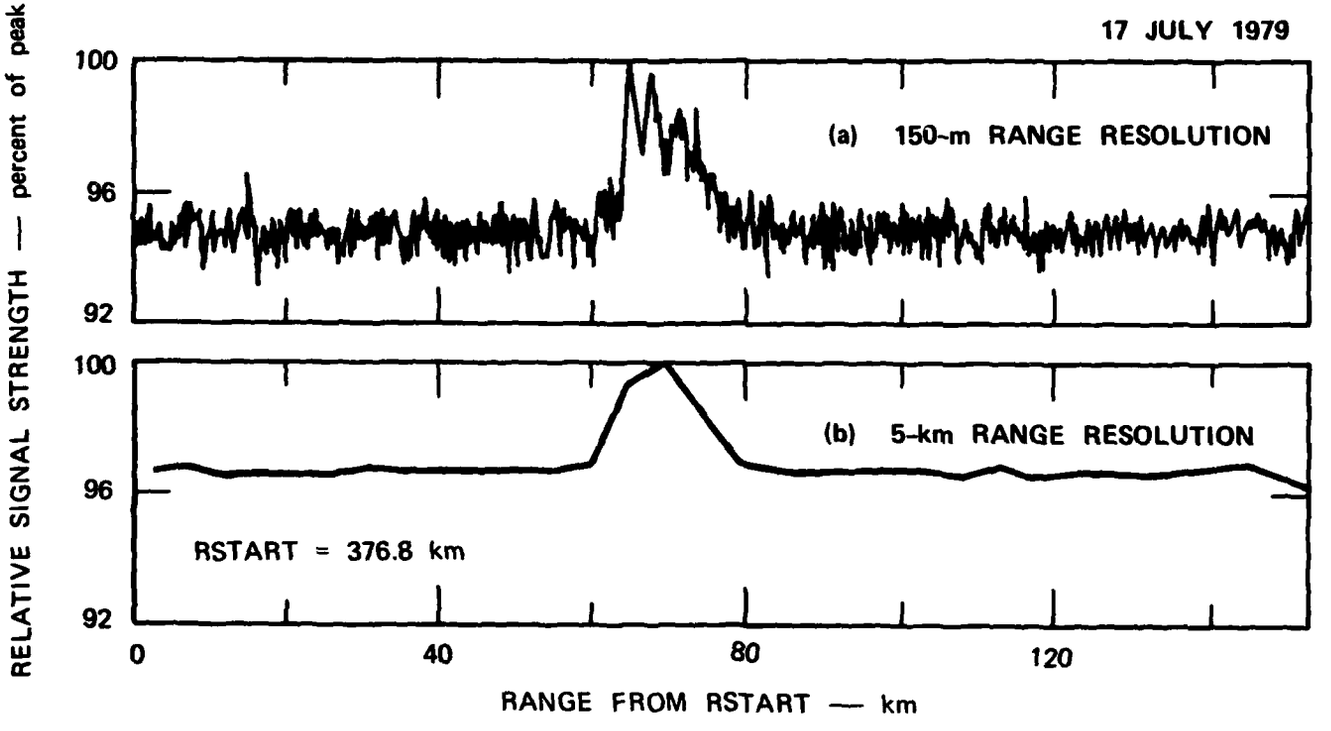

FIGURE 2 RANGE-POWER PROFILE OF L-BAND BACKSCATTER OBTAINED FROM 11-cm FAI

approximately 5 km. Backscatter extends in range from 437 km to 457 km with a peak in backscatter strength located at 447 km. Peak backscatter strength is about -46 dBsm. The noise level is only a fraction of a dB below the peak in spread-F backscatter.

Despite the small signal-to-noise ratio, it is clear from Figure 2 that backscatter from 11-cm FAI was indeed detected with TRADEX. There is no remaining doubt when we note the spatial collocation (Figure 1) of the L-band backscatter with one of the strongest backscatter regions found in the plume at both UHF and VHF.

To compare the TRADEX measurement with those by ALTAIR, we must convert the -46 dBsm discrete target cross section into volume reflectivity. If we assume that the radar scattering volume is filled with FAI, we obtain a value of about 5×10^{-15} m^2/m^3, which is approximately 32 dB above IS levels (for an electron density of 10^6 el/cm^3.) The extent to which the scattering volume is actually filled is dependent on the magnetic aspect sensitivity of equatorial FAI. The filled volume approximation is obviously less valid with increasing radar beamwidth. Using the same assumption (filled scattering volume) for the VHF and UHF data, we can estimate a wavelength dependence of FAI strength. We find that the wavelength dependence between L band and UHF to be $\lambda^{1.3}$ and that between UHF and VHF to be $\lambda^{2.3}$

The implication that the power-law spectral index decreases at the shorter spatial wavelengths is important if shown to be real. Rough estimates to correct for magnetic aspect sensitivity and unscaled antenna beamwidths indicate that although the spectral index does increase, there remains a decrease in the spectral index at shorter FAI wavelengths. Results of a more complete analysis of the wavelength dependence of small-scale FAI will be presented in a future paper.

V DISCUSSION AND CONCLUSIONS

We have described the first observations of radar backscatter from 11-cm FAI. The preliminary results on 36-cm and 11-cm FAI appear to be consistent with the theoretical model for high-frequency drift waves [Huba et al. 1978]. Backscatter has now been observed on either side of the frequency at which maximum backscatter might be expected on the basis of the condition, $kr_e \sim 1$. The relatively flat wavelength dependence implied by the results ($\lambda^{1.3}$)--if proven accurate--supports the idea that the driving point is indeed $kr_e \sim 1$.

If these small-scale FAI are indeed produced by high-frequency drift waves, the occurrence of 11-cm FAI might very well be unique to the equatorial ionosphere. A more generalized analysis of the high-frequency drift wave theory [Huba and Ossakow, 1979; Goldman and Sperling, 1979] has shown that viscous damping of the electrons (via electron-electron collisions) will damp out the instability for cases in which the electron density is much greater than 10^4 el/cm^3 (for a moderate electron-density gradient). On this basis, 11-cm FAI will occur primarily within the equatorial plasma bubbles where the electron densities are low. Whether FAI with much smaller spatial wavelengths can exist even in the equatorial case depends on the existence of steeper electron density gradients and the Debye length effects.

The requirement of low electron density will preclude the presence of small-scale FAI (via high-frequency drift waves) in barium ion clouds. Although the striations in barium clouds are initiated by the gradient-drift instability (e.g., Linson and Workman, [1970]), which is a direct analog of the Rayleigh-Taylor instability that initiates equatorial spread F (e.g., Ossakow and Chaturvedi [1978]), both the striations and the background ionosphere (into which the barium cloud is injected) have higher electron densities than required to trigger high-frequency drift waves. This conclusion is consistent with

available experimental evidence. Bates [1969] operated step-frequency sounders in Alaska as part of the Secede III barium release program. Using oblique-incidence backscatter sounders that operated between 4 MHz and 64 MHz, backscatter was found occurring up to a frequency near 45 MHz, with a maximum in backscatter strength around 30 MHz. (Of course, we do not know what a more sensitive radar would have seen.)

Aside from the consideration of the source mechanism, the observation of 11-cm FAI is also noteworthy because it represents detection of FAI with a spatial wavelength that is closer to the electron gyroradius and, possibly, also closer to the Debye length than any other measurement of ionospheric FAI. As discussed in Section II, 11-cm FAI in the equatorial ionosphere is within a factor of 3 of the electron gyroradius and perhaps as close as a factor of 1.5 of the Debye length.

The only observations of ionospheric FAI that approaches the measurements reported here were those made at 3000 MHz from auroral electrojet irregularities [Chesnut et al., 1968]. Although the radar frequency for the auroral backscatter measurements is a factor of 2.3 higher than that used in this experiment, the ratios of FAI wavelength to electron gyroradius and of FAI wavelength to Debye length are larger than found in this experiment. The reason is that auroral backscatter occurs in the E layer in which the electron temperature is lower than in the F layer, and in polar region where the magnetic flux density is higher than in the equatorial region. Typical E-region electron densities are also higher than those in plasma bubbles.

In the auroral case, the electron gyroradius for an electron temperature of 300K is 1 cm. The FAI wavelength (5 cm) is, therefore, a factor of 5 greater than the electron gyroradius. There are, of course, conditions of intense particle precipitation during which the electron temperature can reach 1200K. In this case, the electron gyroradius is 2 cm and the factor drops to 2.5, which is slightly smaller than for the equatorial results. However, Tsunoda and Presnell [1976] have shown that the conditions for FAI growth via the two-stream instability (source mechanism for E-region electrojet FAI) is not favorable

when the E-region conductivity is high (because of particle precipitation) or when the electron temperature is high. High conductivity tends to short out the ionospheric electric field that drives the two-stream instability. High temperatures also inhibit two-stream growth because they raise the ion-acoustic speed, which controls the instability threshold. Therefore, *if we allow high electron temperatures*, we introduce difficulties in FAI generation via the two-stream instability.

In the auroral case, the Debye length is also smaller because of lower electron temperatures and higher electron densities. For example, for an electron temperature of 300K and an electron density of 10^5 el/cm^3, the Debye length is 0.38 cm. For an electron density of 10^6 el/cm^3, the Debye length decreases to 0.12 cm. The ratio of FAI wavelength to Debye length is, therefore, between 13 and 42 for the auroral case. For the equatorial case, the Debye length can range between 3.3 cm and 2.2 cm for electron densities between 10^3 el/cm^3 and 10^4 el/cm^3. The ratio of FAI wavelength to Debye length, therefore, ranges between 1.5 to 5.

REFERENCES

Bates, H. F., Step frequency radar study of Secede III barium release, Final Report, DASA 2409, Contract DASA01-69-C-0032-P001, SRI Project 7784, Stanford Research Institute, Menlo Park, CA (1969).

Basu, S., S. Basu, and B. K. Khan, Model of equatorial scintillations from in-situ measurements, Radio Sci., 11, 821-832, 1976.

Booker, H. G. and W. H. Wells, Scattering of radio waves by the F region of the ionosphere, Terr. Magn. Atmos. Electr., 43, p. 249, 1938.

Chesnut, W. G., J. C. Hodges, and R. L. Leadabrand, Auroral backscatter wavelength dependence studies, Final Report, Contract AF 30(602)-3734, SRI Project 5535, Stanford Research Institute, Menlo Park, CA (1968).

Clemesha, B. R., An investigation of the irregularities in the F region associated with equatorial type spread F, J. Atmos. Terr. Phys., 26, p. 91, 1964.

Farley, D. T., B. B. Balsley, R. F. Woodman, and J. P. McClure, Equatorial spread F: Implications of VHF radar observations, J. Geophys. Res., 75, p. 7199, 1970.

Goldman, S. R. and J. L. Sperling, Aspects of late-time striation behavior and satellite communication effects, Final Report, DNA 4923F, Contract DNA001-76-C-0186-P00005, JAYCOR, Del Mar, CA (1979).

Hanson, W. B. and S. Sanatani, Large Ni gradients below the equatorial F peak, J. Geophys. Res., 78, p. 1167, 1973.

Huba, J. D. and S. L. Ossakow, Destruction of cyclotron resonances in weakly collisional, inhomogeneous plasmas, Phys. Fluids, 22, p. 1349, 1979.

Huba, J. D., P. K. Chaturvedi, S. L. Ossakow, and D. M. Towle, High frequency drift waves with wavelengths below the ion gyroradius in equatorial spread F, Geophys. Res. Lett., 5, p. 695, 1978.

Kelleher, R. F. and N. J. Skinner, Studies of F region irregularities at Nairobi, II-By direct backscatter at 27.8 MHz, Ann. Geophys., 27, p. 195, 1971.

Linson, L. M. and J. B. Workman, Formation of striations in ionospheric plasma clouds, J. Geophys. Res., 75, p. 3211, 1970.

McClure, J. P., W. B. Hanson, and J. H. Hoffman, Plasma bubbles and irregularities in the equatorial ionosphere, J. Geophys. Res., 82, p. 2650, 1977.

Ossakow, S. L. and P. K. Chaturvedi, Morphological studies of rising equatorial spread F bubbles, J. Geophys. Res., 83, p. 2085, 1978.

Szuszczewicz, E. P., R. T. Tsunoda, R. Narcisi, and J. C. Holmes, Coincident radar and rocket observations of equatorial spread F, submitted to Geophys. Res. Lett., 1980.

Towle, D. M., VHF and UHF radar observations of equatorial F region ionospheric irregularities and background densities, Radio Sci., 15, p. 71, 1980.

Tsunoda, R. T., On the spatial relationship of 1-m equatorial spread-F irregularities and plasma bubbles, J. Geophys. Res., 85, p. 185, 1980a.

Tsunoda, R. T., Magnetic-field-aligned characteristics of plasma bubbles in the nighttime equatorial ionosphere, accepted for publication, J. Atmos. Terr. Phys., 1980b.

Tsunoda, R. T., Time evolution and dynamics of equatorial backscatter plumes--1. Growth phase, submitted to J. Geophys. Res., 1980c.

Tsunoda, R. T. and R. I. Presnell, On a threshold electric field associated with the 398-MHz diffuse radar aurora, J. Geophys. Res., 81, p. 88, 1976.

Tsunoda, R. T., M. J. Baron, J. Owen, and D. M. Towle, Altair: An incoherent scatter radar for equatorial spread-F studies, Radio Sci., 14, p. 1111, 1979.

Woodman, R. F. and S. Basu, Comparison between in-situ spectral measurements of F-region irregularities and backscatter observations at 3-m wavelength, Geophys. Res. Lett., 5, p. 869, 1978.

Woodman, R. F. and C. La Hoz, Radar observations of F-region equatorial irregularities, J. Geophys. Res., 81, p. 5447, 1976.

DISTRIBUTION LIST

DEPARTMENT OF DEFENSE

Assistant Secretary of Defense
Comm, Cmd, Cont & Intell
ATTN: C3IST&CCS, M. Epstein
ATTN: Dir of Intell Sys, J. Babcock

Assistant to the Secretary of Defense
Atomic Energy
ATTN: Executive Assistant

Defense Advanced Rsch Proj Agency
ATTN: TIO

Defense Communications Agency
ATTN: Code 101B
ATTN: Code 205
ATTN: Code 480, F. Dieter

Defense Communications Engineer Center
ATTN: Code R410, R. Craighill
ATTN: Code R123

Defense Nuclear Agency
3 cy ATTN: RAAE
4 cy ATTN: TITL

Defense Technical Information Center
12 cy ATTN: DD

Field Command
Defense Nuclear Agency
ATTN: FCPR

Field Command
Defense Nuclear Agency
Livermore Division
ATTN: FCPRL

Interservice Nuclear Weapons School
ATTN: TTV

Joint Chiefs of Staff
ATTN: C3S Evaluation Office

Undersecretary of Def for Rsch & Engrg
ATTN: Strategic & Space Systems (OS)

WWMCCS System Engineering Org
ATTN: R. Crawford

DEPARTMENT OF THE ARMY

Atmospheric Sciences Laboratory
U.S. Army Electronics R&D Command
ATTN: DELAS-EO, F. Niles

BMD Advanced Technology Center
Department of the Army
ATTN: ATC-T, M. Capps
ATTN: ATC-R, D. Russ
ATTN: ATC-O, W. Davies

BMD Systems Command
Department of the Army
ATTN: BMDSC-HW

DEPARTMENT OF THE ARMY (Continued)

Harry Diamond Laboratories
Department of the Army
ATTN: DELHD-N-P
ATTN: DELHD-N-P, F. Wimenitz
ATTN: DELHD-I-TL, M. Weiner

U.S. Army Materiel Dev & Readiness Cmd
ATTN: DRCLDC, J. Bender

U.S. Army Missile Intelligence Agency
ATTN: J. Gamble

U.S. Army Nuclear & Chemical Agency
ATTN: Library

U.S. Army Satellite Comm Agency
ATTN: Document Control

U.S. Army TRADOC Systems Analysis Activity
ATTN: ATAA-PL

DEPARTMENT OF THE NAVY

Naval Electronic Systems Command
ATTN: PME-117-2013, G. Burnhart
ATTN: PME-117-211, B. Kruger
ATTN: Code 501A
ATTN: PME-117-20

Naval Research Laboratory
ATTN: Code 4780, S. Ossakow
ATTN: Code 4700, T. Coffey

Naval Surface Weapons Center
ATTN: Code F31

Office of Naval Research
ATTN: Code 465

Strategic Systems Project Office
Department of the Navy
ATTN: NSP-43
ATTN: NSP-2722, F. Wimberly

DEPARTMENT OF THE AIR FORCE

Air Force Geophysics Laboratory
ATTN: OPR, A. Stair
ATTN: OPR, H. Gardiner
ATTN: PHI, J. Buchau
ATTN: PHP, J. Mullen

Air Force Weapons Laboratory
Air Force Systems Command
ATTN: DYC
ATTN: SUL

Air Force Wright Aeronautical Laboratories
ATTN: AAD, W. Hunt
ATTN: A. Johnson

Ballistic Missile Office
Air Force Systems Command
ATTN: MNNH, M. Baran

DEPARTMENT OF THE AIR FORCE (Continued)

Deputy Chief of Staff
Research, Development, & Acq
Department of the Air Force
ATTN: AFRDQ

Headquarters Space Division
Air Force Systems Command
ATTN: SKA, M. Clavin

Headquarters Space Division
Air Force Systems Command
ATTN: SZJ
ATTN: SZJ, W. Mercer

Headquarters Space Division
Air Force Systems Command
ATTN: E. Butt

Strategic Air Command
Department of the Air Force
ATTN: XPFS
ATTN: NRT

DEPARTMENT OF ENERGY CONTRACTORS

EG&G, Inc
ATTN: D. Wright
ATTN: J. Colvin

Lawrence Livermore National Laboratory
ATTN: L-31, R. Hager
ATTN: L-389, R. Ott

Los Alamos National Scientific Laboratory
ATTN: E. Jones
ATTN: D. Simons
ATTN: MS 664, J. Zinn
ATTN: MS 670, J. Hopkins

Sandia National Laboratories
ATTN: Org 4241, T. Wright
ATTN: Org 1250, W. Brown

OTHER GOVERNMENT AGENCY

Institute for Telecommunications Sciences
National Telecommunications & Info Admin
ATTN: W. Utlaut

DEPARTMENT OF DEFENSE CONTRACTORS

Aerospace Corp
ATTN: D. Olsen
ATTN: V. Josephson
ATTN: N. Stockwell

APTEK
ATTN: T. Meagher

Berkeley Research Associates, Inc.
ATTN: J. Workman

Charles Stark Draper Lab, Inc
ATTN: D. Cox
ATTN: J. Gilmore

ESL, Inc
ATTN: J. Marshall

DEPARTMENT OF DEFENSE CONTRACTORS (Continued)

General Electric Co
ATTN: A. Harcar
ATTN: M. Bortner

General Electric Company—TEMPO
ATTN: M. Stanton
ATTN: DASIAC
ATTN: T. Stevens
ATTN: W. Knapp
ATTN: W. McNamara

General Research Corp
ATTN: J. Ise, Jr
ATTN: J. Garbarino

Sylvania System Group
ATTN: M. Cross

HSS, Inc
ATTN: D. Hansen

Institute for Defense Analyses
ATTN: E. Bauer

JAYCOR
ATTN: S. Goldman

Johns Hopkins University
ATTN: T. Potemra

Lockheed Missiles & Space Co, Inc
ATTN: D. Churchill

M.I.T. Lincoln Lab
ATTN: D. Towle

Martin Marietta Corp
ATTN: R. Heffner

McDonnell Douglas Corp
ATTN: R. Halprin
ATTN: G. Mroz
ATTN: W. Olson

Meteor Communications Consultants
ATTN: R. Leader

Mission Research Corp
ATTN: D. Sappenfield
ATTN: D. Sowle
ATTN: R. Bogusch
ATTN: R. Hendrick
ATTN: R. Kilb
ATTN: F. Fajen
ATTN: S. Gutsche

Mitre Corp
ATTN: B. Adams

Mitre Corp
ATTN: J. Wheeler
ATTN: W. Foster
ATTN: W. Hall

Photometrics, Inc
ATTN: I. Kofsky

DEPARTMENT OF DEFENSE CONTRACTORS (Continued)

Physical Dynamics, Inc
ATTN: E. Fremouw

R & D Associates
ATTN: C. MacDonald
ATTN: F. Gilmore
ATTN: W. Karzas
ATTN: R. Lelevier
ATTN: B. Gabbard
ATTN: P. Haas

R & D Associates
ATTN: B. Yoon

Rand Corp
ATTN: C. Crain
ATTN: E. Bedrozian

Science Applications, Inc
ATTN: L. Linson
ATTN: D. Hamlin

Science Applications, Inc
ATTN: J. Cockayne

Technology International Corp
ATTN: W. Boquist

DEPARTMENT OF DEFENSE CONTRACTORS (Continued)

SRI International
ATTN: G. Smith
ATTN: C. Rino
ATTN: W. Jaye
ATTN: M. Baron
ATTN: R. Leadabrand
ATTN: W. Chesnut
10 cy ATTN: R. Tsunoda

TRW Defense & Space Sys Group
ATTN: R. Plebuch

Utah State University
ATTN: K. Baker, UMC-41, Elec Eng Dept
ATTN: Larson
ATTN: J. Dupnik

Visidyne, Inc
ATTN: J. Carpenter
ATTN: C. Humphrey

University of California at San Diego
ATTN: H. Booker


DA
FILM